JWMM

First-Flush Driven Sediment Graph Modeling with Soil Moisture Accounting

S.A. Siddiqui[1], P.R. Patil[2], S.K. Mishra[3], S.K. Jain[3], and S. Kumar[1] (2025)

[1]*Graphic Era (Deemed to be University) Uttarakhand, India;*

[2]*National Institute of Hydrology, Uttarakhand, India;*

[3]*Indian Institute of Technology, Uttarakhand, India*

DOI: https://doi.org/10.14796/JWMM.H552

ABSTRACT

The first-flush is the initial surge of highly concentrated mass of pollutants in storm runoff, mobilizing mass accumulated on land surface after dry periods. Like initial abstraction (I_a) in hydrology—which is water lost through interception, infiltration, evaporation, and surface depression storage and does not contribute to immediate surface runoff—the first-flush also appears at the watershed outlet but isn't a true sediment loss. It is crucial for designing on-site treatment facilities, allowing efficient isolation, storage, and treatment of stormwater in small catchments. Neglecting the first-flush may underestimate early-stage erosion. Developing sediment yield and graph models (SYMs and SGMs) is challenging due to nonlinearity of rainfall-runoff-sediment transport, unrealistic inputs, parameter sensitivities, oversimplified processes, landscape heterogeneity, human impacts, and data limitations. The SYMs predict total sediment load, while SGMs capture its temporal variation. Integrating the first flush with conventional SGM improves its accuracy and reliability by considering loose surface debris, and prior land use. The proposed improved first-flush driven sediment graph model with soil moisture accounting (IFF-SMA-SGM) couples the first-flush concept with the soil conservation service-curve number (SCS-CN) method (now the natural resource conservation service (NRCS) curve number method), power law, and Nash's instantaneous unit sediment graph (IUSG) approach. It considers initial or existing soil moisture (V_0) and I_a to work out the sediment yield. The model was calibrated and validated using a total of 16 sediment graphs (in an 8:8 ratio) recorded at Sub-watershed 6 (W6), Sub-watershed 7 (W7), and Sub-watershed 14 (W14), in the Goodwin Creek (GC) experimental watersheds in Oxford, Mississippi, USA, and the Mansara watershed in Uttar Pradesh, India. The model closely replicated the observed sediment graphs during both calibration and validation, demonstrating strong agreement in peak sediment load (Q_{PS}), total sediment load (Q_S), and time to peak sediment load (t_{PS}). The model demonstrated high efficiency across most calibration and validation events, reflecting strong alignment between

---

Siddiqui, S.A., P.R. Patil, S.K. Mishra, S.K. Jain, and S. Kumar. 2025. "First-Flush Driven Sediment Graph Modeling with Soil Moisture Accounting." *Journal of Water Management Modeling* 33: H552. https://doi.org/10.14796/JWMM.H552 www.chijournal.org ISSN: 2292-6062 © Siddiqui et al. 2025

This work is licensed under a Creative Commons Attribution 4.0 International License

simulated and observed sediment yields. This study also highlights the IFF-SMA-SGM model's strong potential for accurate sediment yield prediction in hydro-meteorologically similar watersheds.

1. INTRODUCTION

Conventional SYMs/SGMs struggle with parameter inconsistencies, unreliable estimates, high errors, limited field applicability, and interpretability issues, leading to inaccurate sediment graph predictions (Batista et al. 2019). This study aims to develop an improved model (i.e. IFF-SMA-SGM) for more accurate and reliable sediment yield estimation. The objectives are to:

1. Integrate the first-flush effect into the conventional SMA-based SGM, and
2. Evaluate the model using actual sediment graphs to enhance parameter consistency, accuracy, and field applicability.

The study incorporates the first-flush phenomenon, IUSG, SCS-CN method, and power law for a more physically plausible and interpretable model.

1.1 Definition of first-flush

The stormwater-runoff process presents a major environmental challenge known as the first-flush phenomenon, where initial runoff pulses carry significantly higher contaminant loads than later steady-state flows (Gupta and Saul 1996; Maestri et al. 1988; Hager 2001; Australia EPA 2006). A small fraction of runoff often transports a disproportionately large share of pollutants, mobilizing surface debris, soil particles, plant residue, resuspended solids, and dissolved contaminants, degrading downstream water quality (Sansalone and Buchberger 1996; Chui 1997; Larsen et al. 1998; Krebs et al. 1999; Stenstrom et al. 2001). Originating in the 1910s (Metcalf and Eddy 1915), the first-flush concept gained prominence during Florida's first non-point source (NPS) program in the mid-1970's and has since been widely studied in runoff from urban (roofs, highways, paths, drains, and parking lots) and agricultural areas. (Barbosa 1999; Li et al. 2007).

1.2 Presence of first-flush

The first-flush phenomenon is more common in small watersheds (<10 ha) and combined sewer networks (Barco et al. 2008) but is rarely observed in large catchments. In large catchments, runoff from distant areas converge slowly at the outlet, and drainage characteristics dilute the first-flush effect (Gupta and Saul 1996). Factors such as prolonged concentration time, low drainage density, unsaturated conditions, high infiltration, spatial rainfall variability, insufficient rainfall, and dilution contribute to this uncertainty. In contrast, small watersheds experience a short time lag, making the first-flush more pronounced. As readily detachable or loose material diminishes, channel and stream bank erosion become dominant, significantly influencing the falling limb of the sediment graph (Wilson et al. 2008; Kuhnle et al. 2008).

1.3 Identification of first-flush

Isolating the first-flush from total runoff provides an effective strategy for controlling water pollution (Su and Mitchell 2003; Sansalone and Cristina 2004; Sansalone 2005; Australia EPA 2006). However, first-flush identification criteria vary widely and lack universal applicability. For instance, in Florida urban sites, the first 25 mm of runoff carried up to 90% of the total contaminant load identified as the first-flush (Schiffer 1989). Typically, 10–20 mm of runoff is isolated, though without strong theoretical or experimental support. Studies have proposed various 'load/volume' ratios for first-flush analysis: 80/20 (Stahre and Urbonas 1990), 40/20 (Deletic 1998), and 50/25 (Bach et al. 2010; Wanielista and Yousef 1993). Saget et al. (1996) found that 30% of initial runoff captured 80% of pollutants, while Bertrand-Krajewski et al. (1998) developed a 'mass/volume' curve for first-flush detection. However, these metrics may not be sufficient across different land uses.

1.4 Utility of first-flush

Identifying, quantifying, and isolating the first flush is crucial for effective stormwater management, pollution control, and ecological protection. Characterizing contaminant peaks and expulsion limits informs the design of on-site facilities like green roofs, bioretention cells, infiltration trenches, vegetated swales, porous pavements, rain barrels, and detention units. It facilitates regulatory compliance to protect aquatic habitats. It also aids in selecting land use-specific best management practices (BMPs) and shaping runoff management policies. However, confirming the first flush requires long-term, continuous event-based streamflow sampling across varying land uses, rainfall intensities and durations to capture the initial surge of sediment-laden runoff, demanding significant resources. This involves deploying auto samplers for time-sequenced water sampling during storm events, using in-situ sensors (turbidity, conductivity, and flow) for real-time monitoring, and conducting manual grab sampling at short intervals during storm onset for laboratory analysis. These methods ensure accurate characterization of first-flush dynamics. Limited event samples and the absence of standardized protocols hinder precise identification. Focusing on sediment load during the first flush, rather than event averages, is essential for understanding pollutant variability and erosion mechanisms.

1.5 Soil erosion and sediment yield assessment

Soil erosion is an irreversible form of land degradation, with suspended sediment serving as a key indicator of watershed health and a major component of total sediment yield (Chow 1964; Graf 1984). However, sediment transport processes remain poorly understood due to complex hydrogeological interactions, storm event uncertainties, data scarcity, and inaccessible sampling sites in extreme conditions (Bennett 1974; Jones et al. 1981; Reid and Frostick 1987; Pilgrim et al. 1988). Field studies are further limited by high costs, large study areas, a lack of skilled personnel or automation, and the risks of data collection during extreme weather events.

Sediments absorb or transport pollutants like heavy metals, nutrients, and chemicals, contributing to eutrophication and disrupting ecosystems. Accurate prediction of storm-mobilized sediment yield is crucial for maintaining water quality and ecological balance. Understanding suspended sediments helps estimate pollutant loads, trace sources, assess impacts, and implement targeted stormwater management to mitigate pollution. The maximum

daily sediment load defines tolerable or safe limits for aquatic vegetation (Fitzgerald et al. 2001; Kuhnle and Wren 2003), informs soil conservation, and aids in designing or operating hydraulic and flood control structures (Mizumura 1989). Temporal sediment flow rates are vital for water quality modeling and designing high-efficiency sediment control structures. Sediment graphs are particularly important when pollutants are toxic at high concentrations, requiring peak flow rate estimation over averages.

Sediment yield assessment largely depends on mathematical models (Harmon and Doe 2001), but their effectiveness is limited by the complexity of sediment transport (Hrissanthou 1998; Chen and Chau 2016). Challenges include over-parameterization, location-specific inputs, unrealistic assumptions, and inadequate applicability documentation. Despite extensive research, no universally accepted sediment estimation method exists (Kothyari et al. 1996, 2002), and modeling limitations persist (Favis-Mortlock et al. 2000). Model robustness is further constrained by reliability issues and validation across different datasets (Jetten et al. 1999). Effective models require comprehensive data for development, execution, and validation (Blöschl and Sivapalan 1995; Jakeman et al. 2006).

Erosion and sediment transport models are classified as empirical, conceptual, or process-based (Merritt et al. 2003; Aksoy and Kavvas 2005; Karydas et al. 2014; Borrelli et al. 2021). Johnson (1943) introduced suspended sediment distribution graphs, similar to hydrographs. Renard and Laursen (1975) computed sediment graphs by multiplying hydrographs with modeled sediment concentrations, but this method is unsuitable for agricultural watersheds as it does not account for source erosion. Bruce et al. (1975) developed a SGM that incorporates soil erosion and transport capacity. The empirical universal soil loss equation (USLE) (Wischmeier and Smith 1978) estimates average annual soil loss from sheet and rill erosion. However, it is region-specific, does not predict event-specific loss, excludes gully and stream bank erosion, oversimplifies rainfall-erosion dynamics, and ignores land use and climate changes. Empirical models often make unrealistic assumptions about catchment physics. Conceptual models, such as the unit sediment graph (USG) (Rendon-Herrero 1978), rely solely on measured data, neglecting watershed cover and conservation practices (Williams 1978).

The instantaneous unit sediment graph (IUSG) (Williams 1978; Singh et al. 1982; Kumar and Rastogi 1987; Lee and Singh 2005) is based on the water budget equation and a linear storage (S) discharge – (Q) relationship. It represents sediment distribution from an instantaneous burst of rainfall producing unit runoff and is derived by multiplying the instantaneous unit hydrograph with the sediment concentration distribution. However, conceptual models have limited representation of physical process. Most sediment graph techniques depend on measured hydrographs, sediment graphs, and additional inputs like rainfall erosivity, storm intensity, and hydrograph time parameters, highlighting their data-intensive nature.

Various IUSG models based on the linear S-Q concept (Nash 1957) have been widely used (Kumar and Rastogi 1987; Sharma et al. 1992; Sharma and Murthy 1996; Gracia-Sanchez 1996; Lee and Singh 1999, 2005; Rai and Mathur 2007; Singh et al. 2008; Bhunya et al. 2010). Raghuwanshi et al. (1994) developed an IUSG-based model incorporating sediment translation and attenuation functions, while Lee and Singh (1999, 2005) integrated IUSG with Kalman filters and Tank models to derive SGMs. However, USG- and IUSG-based SGMs often depend on regression relationships with effective rainfall to estimate mobilized sediment, making them less reliable. These models also fail to explicitly incorporate key physical parameters influencing

runoff and sediment yield, such as soil and land use types, hydrologic conditions, and antecedent moisture, despite their complex structure.

The integration of USLE and the SCS-CN method (Mishra et al. 2006) improved hydrological representation by considering I_a and V_0 but could not predict temporal sediment yield. Singh et al. (2008) and Bhunya et al. (2010) combined the SCS-CN method, power law, and IUSG to develop conceptual SGMs, while Tyagi et al. (2008) used an SCS-CN-based infiltration model to compute rainfall-excess rates and a proportionality concept for sediment-excess estimation. Lee and Yang (2010) coupled geomorphological IUSG with kinetic wave models to develop time-distributed SYMs. However, these models lack soil moisture accounting. To address this, Gupta et al. (2019) introduced SMA-based SGMs incorporating soil moisture storage from the GR4J (Génie Rural à 4 paramètres Journalier) runoff model (Perrin et al. 2003), the SCS-CN method, power law, and IUSG, assuming that for a saturated soil rainfall equals runoff (Michel et al. 2005). In the GR4J model, soil moisture is defined as the difference between available moisture and field capacity, naturally transitioning from saturation to field capacity within 2–4 days, following drainage. Unlike natural systems, the GR4J model does not require saturation as the upper limit, improving its effectiveness in rainfall-runoff simulations. Modern tools like the U.S. environmental protection agency-storm water management model (USEPA-SWMM) effectively simulate stormwater runoff and quality, allowing for first-flush analysis. However, an analytical approach for sediment event processing remains necessary. To bridge these gaps, this study proposes a theoretically improved model (IFF-SMA-SGM), incorporating physical variables and re-parameterizing the SMA-based SGM. The model is applied to first-flush sediment graphs from experimental watersheds in the U.S. and India, and validated with alternative datasets of these watersheds, enhancing its reliability, significance, and adaptability for urban development and environmental protection.

2. MATERIALS AND METHODS

The proposed IFF-SMA-SGM integrates the first-flush concept, sediment delivery ratio, power law, SCS-CN method, and Nash's IUSG, with the following key assumptions:

1. Negligible bed load contributions – total sediment yield is assumed to be equal to suspended sediment yield,
2. Effective rainfall (P_e) increases linearly with time t, thus $P_e = i_e \cdot t$, with i_e as uniform effective rainfall intensity (mm/hr),
3. Inflow is instantaneous and uniformly distributed over the watershed, producing one unit of mobilized sediment, and
4. Linear and time-invariant process.

These approaches or concepts were chosen for their proven effectiveness in modeling runoff generation, sediment transport, and event-based sediment dynamics. Mobilized sediment is estimated using the SCS-CN method and power law, incorporating rainfall intensity, soil type, land use, hydrologic conditions, and antecedent soil moisture. This approach makes the model more physically realistic than conventional regression-based models. The mobilized sediment is then routed through a cascade of linear reservoirs (Nash 1957), and sediment graphs are derived by convolving Nash's IUSG with mobilized sediment.

2.1 SCS-CN proportionality and power law

The SCS-CN proportionality concept is given in Equation 1 as:

$$\frac{Q}{(P-I_a)} = \frac{F}{S} \quad (1)$$

Where:

Q = direct runoff,

P = total rainfall,

I_a = initial abstraction,

F = cumulative infiltration excluding I_a,

S = potential maximum retention (ranges from 0 to ∞) = (25,400/CN) – 254, and

CN = curve number.

Potential maximum storage is the initial storage space available for water retention, which depends on soil porosity and the initial soil moisture content. *F* can also be assumed as the dynamic portion of infiltration. As *Q* approaches $P - I_a$, *F* tends towards *S*. The $I_a = \lambda \cdot S$ includes short-term initial losses: evaporation, interception, surface detention, and infiltration. Here, I_a / S yields λ, which varies with climatic conditions and ranges from 0 to infinity. The *CN* is determined from SCS (1972) tables based on catchment characteristics such as soil type, land use, hydrologic conditions, and initial soil moisture. A higher *CN* indicates a greater runoff coefficient (*C*), meaning higher runoff potential for the watershed, and vice versa.

For $I_a = 0$ (immediate ponding), the SCS proportionality (Equation 1) equates $C = Q/P$ to the degree of saturation $S_r = F/S$. This proportional equality ($C = S_r$) can be extended to sediment yield studies by assuming $C = S_r = SDR$ (sediment delivery ratio), as all three equated variables range from 0 to 1 (Mishra et al. 2006). Novotny and Olem (1994) proposed a dimensionless $SDR = Y/A$, which is expressed as a power function of the runoff coefficient, as:

$$SDR = \frac{Y}{A} = \alpha \cdot (C)^{\beta} = \alpha \cdot \left(\frac{Q}{P}\right)^{\beta} \quad (2)$$

Where:

Y = sediment yield,

A = total potential erosion in a particular watershed, and

α and β = empirical coefficients that vary based on watershed characteristics.

The *SDR* serves as a scaling parameter ranging from 0 to 1, generally decreasing with increasing basin size (Roehl 1962). Correlation between *SDR* and *C* (Novotny and Olem 1994) highlights the influence of infiltration and hydrologic losses on *SDR* magnitude. Several factors, including rainfall impact, overland flow energy, vegetation, infiltration, ponding storage, slope variations, and drainage characteristics, significantly affect *SDR* (Novotny et al. 1979, 1986; Novotny 1980; Novotny and Chesters 1981). The power law is widely applied across disciplines, including:

1. Hydrology: Manning's equation, stage–discharge relationships (rating curves), *SDR–C* relationships (Novotny and Olem 1994), empirical peak flow estimation approaches (e.g., Dickens, Ryve's, and Inglis formulas), and suction-moisture content relationships (Mishra and Singh 2003);
2. Ecology: metabolic scaling (Kleiber's Law); and
3. Structural Engineering, Aerospace Engineering, and Metallurgy: Fracture mechanics/crack growth modeling (Paris' Law) to describe particle-size distribution. Its broad applicability underscores the power law's effectiveness in modeling natural and engineering processes.

2.2 Coupling of first-flush

The first-flush reaches the watershed outlet at the onset of a storm when initial losses are met. However, this does not imply an actual loss of sediments. Using the second hypothesis of the SCS-CN method ($I_a = \lambda \cdot S$), Mishra et al. (2006) defined first-flush as $I_f = \lambda_1 \cdot A$, leading to a modified *SDR* as:

$$SDR = \frac{Y-(\lambda_1 \cdot A)}{A-(\lambda_1 \cdot A)} \tag{3}$$

Where:

λ_1 = first-flush coefficient.

2.3 First-flush driven SGM with SMA

By coupling the initial-flush-based *SDR* expression (Equation 3) with the power law (Equation 2), we derive storm-mobilized sediment, Y (kN/km^2):

$$Y = \alpha \cdot (A - \lambda_1 A) \cdot \left(\frac{Q}{P}\right)^{\beta} + \lambda_1 \cdot A \tag{4a}$$

For non-zero I_a, as well as initial soil moisture ($V_0 = \theta S$), the SCS-CN based expression of runoff coefficient proposed by Gupta et al. (2019) is given as:

$$C = \frac{Q}{P} = \frac{V_0 \cdot (P+S) + (P \cdot S)}{(P+S) \cdot (S+V_0+I_a)} \tag{4b}$$

Substituting the Equation 4b in Equation 4a, the total mobilized sediment Y_T (kN) over a given watershed area A_W (km^2) is derived as:

$$Y_T = \alpha \cdot (A - \lambda_1 \cdot A) \cdot A_w \cdot \left[\frac{\theta \cdot (1+k \cdot t) + (k \cdot S \cdot t)}{(1+k \cdot t)(1+\theta+\lambda)}\right]^{2\beta} + (\lambda_1 \cdot A \cdot A_w) \tag{5}$$

Integrating the Horton infiltration equation (Horton 1939) yields the cumulative infiltration as: $F = (f_0 - f_C)/k$ as time, $t \to \infty$. Where, f_0 and f_C are the initial and final infiltration rates (mm/hr) and k is the Horton's decay constant (1/hr). As $Q \to (P - I_a)$, it follows that $F \to S$, thus $S = (f_0 - f_C)/k$, which is crucial for deriving SCS-CN-based infiltration and runoff models. For a typical infiltration data set, f_0 can be assumed equal to the uniform rainfall intensity (i), then $(f_0 - f_C) = (i - f_C) = i_e = S \cdot k$. An assumption that P_e grows linearly with time in Equation 5, leads to

$P_e = i_e \cdot t = k \cdot S \cdot t$. This assumption aligns with infiltration rates obtained from field or laboratory tests and supports the general notion that rainfall grows unbounded (Ponce and Hawkins 1996).

The time-distributed (temporally varied) rainstorm-generated sediment yield at the basin outlet, or the sediment graph (*kN*/hr), is obtained by convolving Nash's IUSG with the total quantity of sediment transported (Y_T). This convolution provides a more realistic representation of sediment yield dynamics during storm events.

$$Q_S(t) = \frac{Y_T(n_S-1)^{n_S}}{[t_{ps}\Gamma(n_S)][(t/t_{ps})e^{-(t/t_{ps})}]^{(n_S-1)}} \quad (6)$$

Bhunya et al. (2003) proposed reliable analytical expressions to determine the shape parameter (n_s) using the known non-dimensional parameter $\beta_s = q_{ps} \cdot t_{ps.}$

$$\begin{cases} n_s = 5.53 \cdot {\beta_s}^{1.75} + 1.04 & \text{for } 0.01 < \beta_s < 0.35 \\ n_s = 6.29 \cdot {\beta_s}^{1.998} + 1.157 & \text{for } \beta_s \geq 0.35 \end{cases} \quad (7)$$

Where:

q_{ps} = peak sediment outflow (1/hr), and

t_{ps} = time to peak sediment outflow (hr).

3. DATA USED

The GC watershed (21.42 km²) in Oxford, Mississippi, USA, managed by the National Sedimentation Laboratory, serves as a research site for erosion studies. This study utilizes rainstorm-generated sediment data from three sub-watersheds: W6-GC (1.25 km²), W7-GC (1.66 km²), and W14-GC (1.66 km²). For model calibration, all four sediment events from W7-GC are used, while all four events from W14-GC are reserved for validation. In W6-GC, a 2:2 ratio is adopted for calibration and validation. Additionally, sediment data from the Mansara watershed (8.70 km²) in Barabanki, U.P., India, monitored under the Indo-German Bilateral Project on Watershed Management, is included, also using a 2:2 calibration-validation split. In total, the proposed eight-parameter IFF-SMA-SGM is calibrated on eight and validated on eight rainstorm-generated sediment events, demonstrating its applicability and reliability.

4. PERFORMANCE EVALUATION

The proposed IFF-SMA-SGM is evaluated using both graphical and statistical methods. For *n* sediment graph ordinates, model performance is assessed using Nash-Sutcliffe Efficiency (NSE), defined as:

$$NSE = \left[1 - \frac{\sum_{i=1}^{n}\left(SG_{Obs,i} - SG_{Comp,i}\right)^2}{\sum_{i=1}^{n}\left(SG_{Obs,i} - \overline{SG_{Obs}}\right)^2}\right] \cdot 100 \quad (8)$$

Where:

SG_{Obs} = observed i^{th} sediment graph ordinate,

SG_{Comp} = computed i^{th} sediment graph ordinate,

$\overline{SG_{Obs}}$ = mean of observed sediment graph ordinates, and

NSE = 100% indicates a perfect model fit.

Additionally, the model's accuracy is quantified using the absolute relative error (*RE*):

$$RE(Q_S \text{ or } Q_{PS} \text{ or } t_{PS}) = \left|\frac{SG_{Obs} - SG_{Comp}}{SG_{Obs}}\right| \cdot 100 \quad (9)$$

Where:

SG_{Obs} = observed sediment graph properties (Q_S or Q_{PS} or t_{PS}),

SG_{Comp} = computed sediment graph properties (Q_S or Q_{PS} or t_{PS}),

$RE(Q_S)$ = *RE* in total sediment load (%),

$RE(Q_{PS})$ = *RE* in peak sediment load (%), and

$RE(t_{PS})$ = *RE* in time to peak sediment load (%).

A lower *RE* indicates a well-performing model, whereas an *RE* close to 100% suggests a poor fit.

5. RESULTS AND DISCUSSION

The rainstorm-generated first-flush coupled temporal sediment rates for the W6-GC, W7-GC, and W14-GC experimental sub-watersheds, along with the Mansara watershed, were calibrated and validated using the proposed IFF-SMA-SGM. Figure 1(a–f) presents the observed and modeled temporal sediment rates (sediment graphs) for the selected calibration and validation events. The calibrated parameters (α, β, k, θ, λ, and λ_1) and their average values used for model validation, along with the observed and computed sediment graph properties (Q_S, Q_{PS}, and t_{PS}), are summarized in Table 1. Model performance was assessed using absolute *REs* for sediment graph properties, while NSE was used to evaluate how well the model-fitted sediment graph aligns with observations (Table 1).

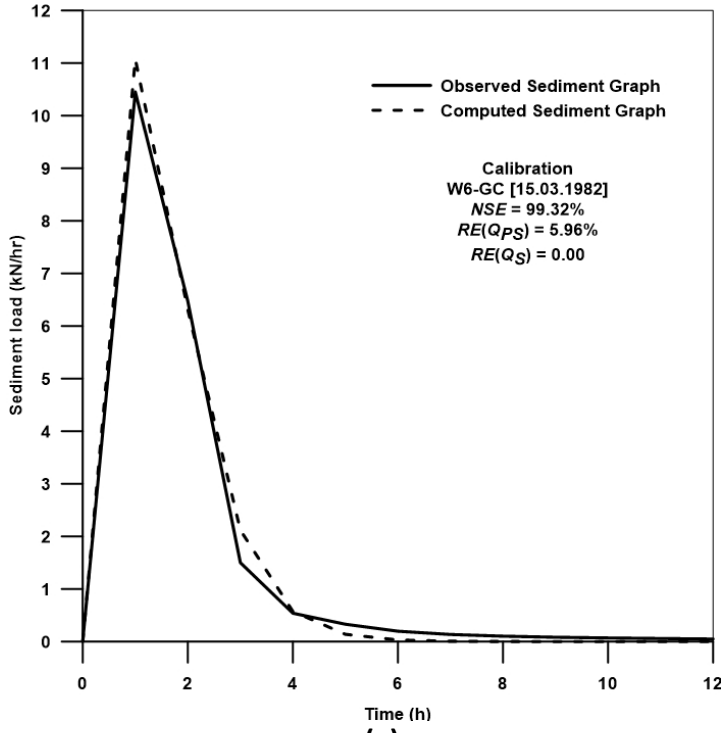
Observed Sediment Graph
Computed Sediment Graph
Calibration
W6-GC [15.03.1982]
NSE = 99.32%
RE(Q_PS) = 5.96%
RE(Q_S) = 0.00
Sediment load (kN/hr)
Time (h)
0
1
2
3
4
5
6
7
8
9
10
11
12

(a)

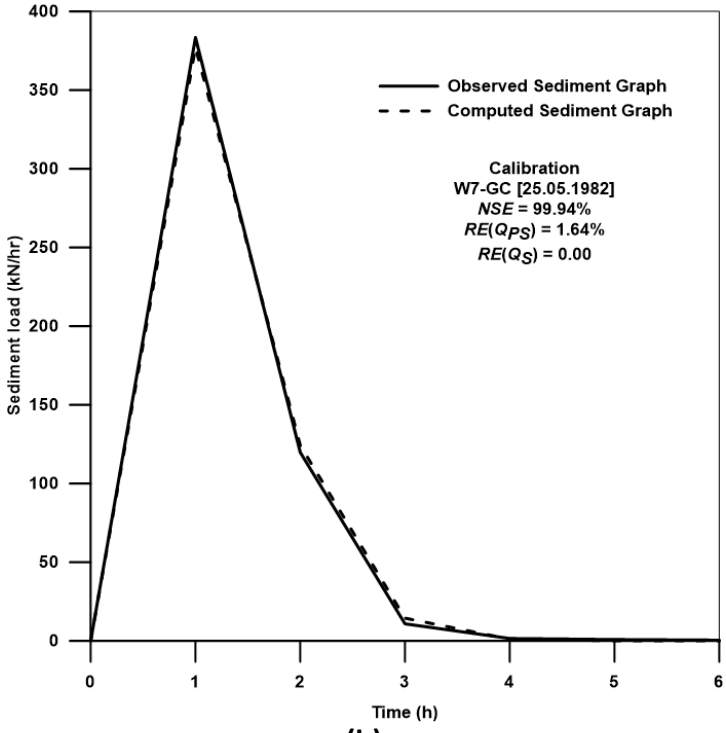
Observed Sediment Graph
Computed Sediment Graph
Calibration
W7-GC [25.05.1982]
NSE = 99.94%
RE(Q_PS) = 1.64%
RE(Q_S) = 0.00
Sediment load (kN/hr)
Time (h)
0
50
100
150
200
250
300
350
400
1
2
3
4
5
6

(b)

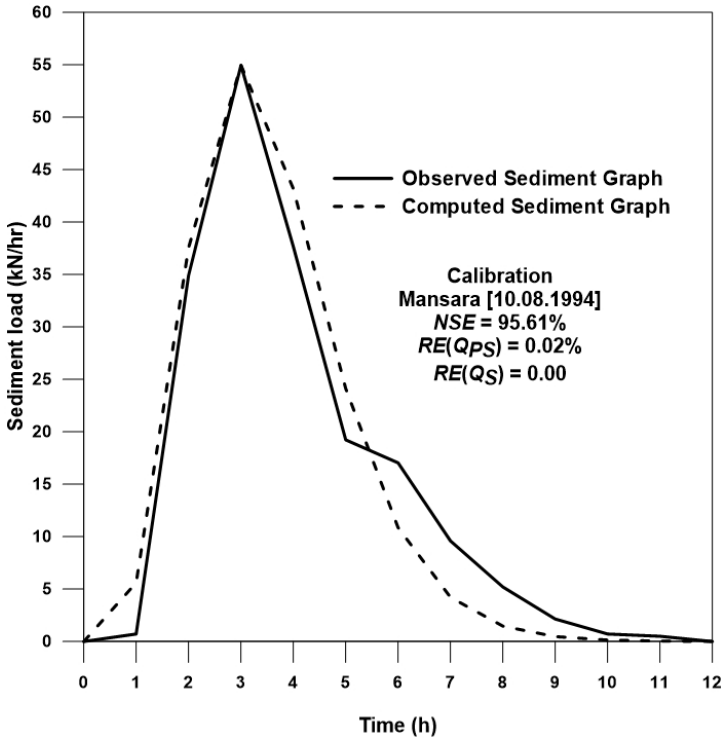
Observed Sediment Graph
Computed Sediment Graph
Calibration
Mansara [10.08.1994]
NSE = 95.61%
RE(QPS) = 0.02%
RE(QS) = 0.00
Sediment load (kN/hr)
Time (h)

(c)

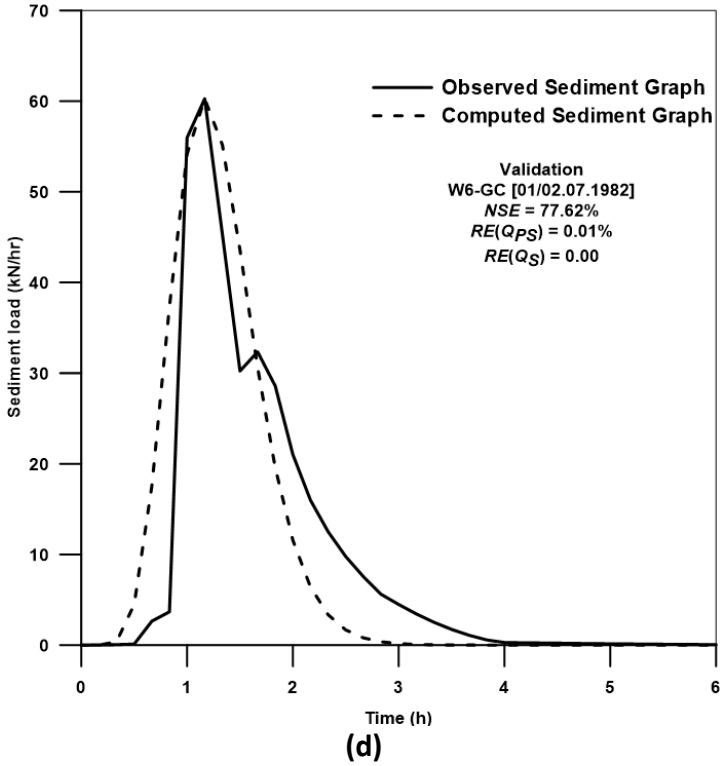
Observed Sediment Graph
Computed Sediment Graph
Validation
W6-GC [01/02.07.1982]
NSE = 77.62%
RE(QPS) = 0.01%
RE(QS) = 0.00
Sediment load (kN/hr)
Time (h)

(d)

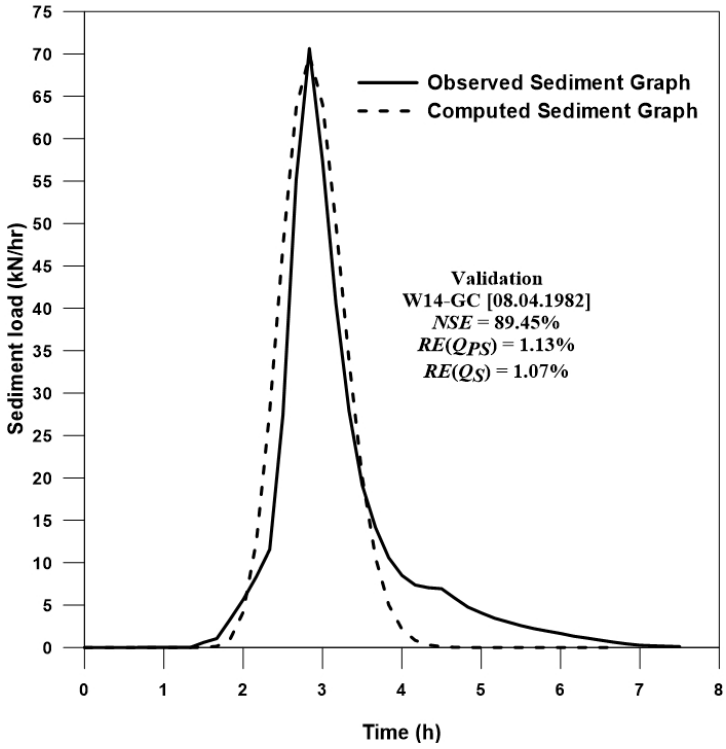

(e)

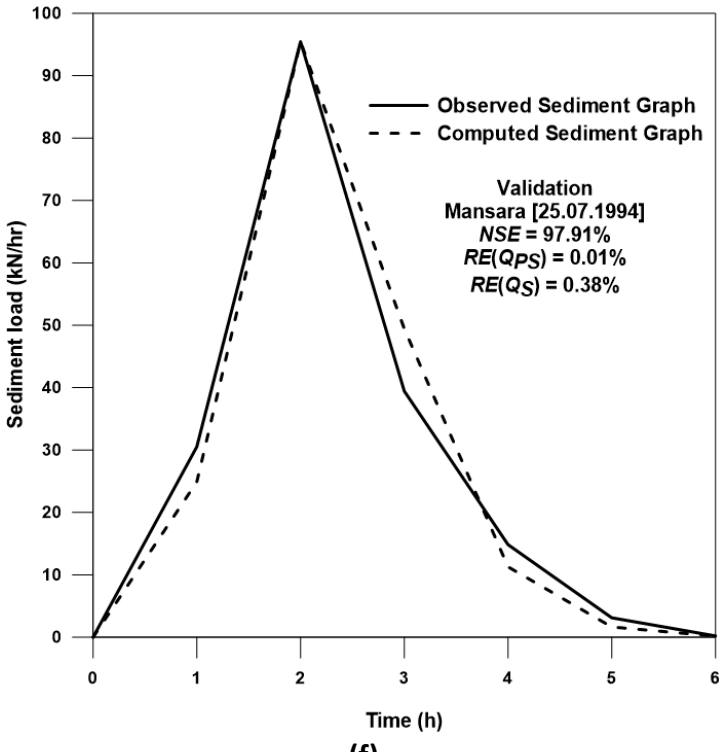

(f)

Figure 1(a-f) Actual and modeled sediment graphs of selected calibration and validation events of study watersheds.

Table 1 Calibration and validation parameters of the model and its statistical performance evaluation using observed and computed SG properties.

Watershed	Event	Parameters							Total sediment outflow Q_S (*kN*)			Peak sediment outflow rate Q_{PS} (*kN*/hr)			Time to peak t_{PS} (hr)			NSE (%)
		α	β	k	θ	λ	λ_1	A	*Obs.*	*Comp.*	*RE* (%)	*Obs.*	*Comp.*	*RE* (%)	*Obs.*	*Comp.*	*RE* (%)	
	Calibration																	
W6	02.01.1982	0.427	0.10	0.04	0.04	0.04	0.02	266.14	183.82	183.82	0.00	155.78	146.65	5.86	1.00	1.00	0.00	98.52
	15.03.1982	0.482	0.10	0.04	0.04	0.04	0.02	29.32	20.25	20.25	0.00	10.45	11.08	5.96	1.00	1.00	0.00	99.32
W7	25.05.1982	0.432	0.10	0.04	0.04	0.04	0.02	581.58	517.06	517.06	0.00	383.45	377.17	1.64	1.00	1.00	0.00	99.94
	03.06.1982	0.428	0.10	0.04	0.04	0.04	0.02	689.34	612.86	612.86	0.00	470.09	457.75	2.62	1.00	1.00	0.00	95.44
	11.08.1982	0.440	0.10	0.04	0.04	0.04	0.02	264.56	235.21	235.21	0.00	282.69	282.53	0.06	2.33	2.33	0.00	39.27
	28.08.1982	0.440	0.10	0.04	0.04	0.04	0.02	3023.59	2688.14	2688.14	0.00	2324.69	2324.87	0.01	1.33	1.33	0.00	59.06
Mansara	10.08.1994	0.284	0.10	0.04	0.04	0.04	0.02	47.03	182.65	182.65	0.00	54.96	54.97	0.02	3.00	3.00	0.00	95.61
	19.07.1994	0.284	0.10	0.04	0.04	0.04	0.02	39.86	154.78	154.78	0.00	63.11	63.09	0.03	3.00	3.00	0.00	89.54
	Validation																	
W6	16.06.1982	0.454	0.10	0.04	0.04	0.04	0.02	98.58	68.09	68.09	0.00	121.30	121.26	0.04	1.17	1.17	0.00	85.62
	02.07.1982	0.454	0.10	0.04	0.04	0.04	0.02	83.87	57.93	57.93	0.00	60.26	60.25	0.01	1.17	1.17	0.00	77.62
W14	18.10.1981	0.435	0.10	0.04	0.04	0.04	0.02	1611.79	1432.98	1417.70	1.07	2800.76	2770.56	1.08	0.67	0.67	0.00	85.32
	08.04.1982	0.435	0.10	0.04	0.04	0.04	0.02	78.36	69.66	68.92	1.07	70.63	69.84	1.13	2.83	2.83	0.00	89.45
	17.07.1982	0.435	0.10	0.04	0.04	0.04	0.02	155.95	138.65	137.11	1.11	282.40	279.37	1.07	0.50	0.50	0.00	87.40
	12.09.1982	0.435	0.10	0.04	0.04	0.04	0.02	82.56	73.40	71.99	1.92	43.03	42.57	1.08	2.00	2.00	0.00	88.32
Mansara	25.07.1994	0.284	0.10	0.04	0.04	0.04	0.02	47.27	183.58	182.89	0.38	95.46	95.45	0.01	2.00	2.00	0.00	97.91
	16.08.1994	0.284	0.10	0.04	0.04	0.04	0.02	94.93	368.64	369.55	0.25	117.34	117.37	0.02	2.00	2.00	0.00	80.19

The proposed model exhibits exceptional performance in fitting sediment graphs for calibration events, achieving the highest NSE of 99.94% for the W7-GC watershed (Figure 1a), followed by 99.32% for W-6 GC (Figure 1b). The NSE for the Mansara watershed drops to 95.61% due to the oscillatory recession limb of the actual sediment graph (Figure 1c). This strong performance is further supported by minimal *REs*(Q_{PS}) of 1.64%, 5.96%, and 0.02%, respectively. For validation events in W6 GC, W14 GC, and Mansara watersheds, the model effectively replicates observed sediment graphs, yielding NSEs of 77.62%, 89.45%, and 97.91%, respectively. These rising NSEs reflect the model's ability to closely match both the rising and recession limbs of actual sediment graphs (Figure 1d-f), despite oscillations in the observed data. The corresponding *REs* (Q_{PS}) of 0.01%, 1.13%, and 0.01%—lower than those in calibration—further validate the model's accuracy in conserving sediment volume over given time base.

By defining the minimization of *RE*(Q_S)—*RE* in total sediment load—as an objective function in the generalized reduced gradient nonlinear programming algorithm (Lasdon et al. 1978), event-wise parameters (α, β, k, θ, λ, λ_1, and A) were calibrated or optimized (Table 1). The objective function aims to replicate the actual peak sediment load while ensuring mass conservation under the sediment graph over a given time base. The peak sediment load governing parameter α varied between 0.284 and 0.482 during calibration across eight selected events from the W6-GC, W7-GC, and Mansara watersheds. In contrast, the other model parameters (β, k, θ, λ, and λ_1) remained constant at 0.10, 0.04, 0.04, 0.04, and 0.02, respectively, during calibration. These parameters exhibited lower sensitivity compared to α, which showed a variation of up to 0.198 between its lowest and highest calibrated values across the W6-GC, W7-GC, and Mansara watersheds.

Horton's decay parameter (k) is defined as the ratio of effective uniform rainfall intensity to potential maximum soil moisture retention (i_e / S) (Mishra and Singh 2003). This implies that k increases as i_e increases, and decreases as S increases or *CN* decreases, and vice versa. The parameter k represents the cumulative influence of multiple physiographic factors, including land use, soil type (hydrologic soil group), rainfall intensity, hydrologic state, antecedent soil moisture (Mein and Larson 1971), slope length, drainage density, and catchment slope. These factors collectively determine the flow-generating potential of a watershed. θ is defined as the ratio (= V_o / S), which ranges between 0 and 1 (Michel et al. 2005). In calibration, it was determined to be 0.04. λ reflects the model's sensitivity to various climatic and surface settings (Ponce and Hawkins 1996). The calibrated value of λ = 0.04 aligns with the recommended threshold of ≤ 0.05 (Hawkins and Khojeini 2000; Woodward et al. 2003). The watershed-specific S is calculated as described in Section 2.1. For model calibration and validation (1981–82) over GC sub-watersheds, S remains constant at 67.52 mm, as the input *CN* = 79 (King et al. 1999) is consistent across all study sites. Similarly, for the model assessment (1994) of the Mansara watershed, both *CN* = 52, and the resulting S = 234.46 mm remain unchanged (Table 1).

By equating the *SDRs* derived from: (i) *SDR* = *Y/A,* and (ii) *SDR* = $0.51 \times A_W^{-0.11}$ (SCS 1972), the event-specific total potential erosion A is calibrated. Its values range from 29.32 *kN*/km² (W6 GC) to 3023.59 *kN*/km² (W7 GC) during calibration. This *SDR*-based approach is also applied during model validation, where A varies from 47.27 *kN*/km² (Mansara) to 1611.79 *kN*/km² (W14 GC) (Table 1). By calibrating A using *SDR* relationships and estimating S using *CN*, other less sensitive model parameters β, k, θ, λ, and λ_1 remain constant across different watersheds or bear identical values irrespective of watershed. Whereas the sensitive parameter α shows only minor variation between its watershed wise lowest and highest calibrated values, as

observed for W6 GC (0.055) and W7 GC (0.012) watersheds, while for the Mansara watershed, α remains constant at 0.284 during calibration. λ_1 represents the proportion of the total sediment load mobilized during the initial phase of a storm event. However, its accurate estimation requires temporal data, obtained through regular sampling of first-flush events across varied land uses, storm intensities, and magnitudes (Table 1).

By maintaining parameter consistency, the IFF-SMA-SGM model minimizes the complexity often associated with conventional calibration, such as unrealistic parameter (α, β, k, θ, λ, A, and S) estimates or sudden jumps in values. This enhances both the physical interpretability and the validity (goodness-of-fit) of the sediment graphs, addressing gaps in conventional sediment yield modeling studies. The IFF-SMA-SGM-based temporal sediment rates closely align with observed sediment rates during both calibration and validation, as confirmed by key sediment graph properties (Q_S, Q_{PS}, and t_{PS}) derived using minimization of $RE(Q_S)$ as the objective function (Table 1). The average calibration parameters (α, β, k, θ, λ, and λ_1) from W6-GC, W7-GC, and Mansara watersheds are then applied to validate the model using sediment events from W6-GC, W14-GC, and Mansara watersheds, respectively. Due to their hydrologic similarity and geographic proximity, the average values of W7-GC calibration parameters are used for validating the model over W14-GC sediment events.

The average calibrated values of α for W6-GC, W7-GC, and Mansara watersheds are 0.454, 0.435, and 0.284, respectively. The other calibrated parameters (β, k, θ, λ, and λ_1) remain consistent across these watersheds, with averaged values 0.10, 0.04, 0.04, 0.04, and 0.02, respectively. These average parameter values were used for validating the model over W6-GC, W14-GC, and Mansara watersheds. Maintaining parameter consistency is crucial for model validation, as inconsistent or widely varying parameters can reduce accuracy and applicability. This issue is particularly critical when applying the model to hydro-meteorologically similar and proximate watersheds (e.g., W14-GC, Figure 1e). The IFF-SMA-SGM approach effectively resolves this challenge, ensuring more representative and reliable sediment yield estimations (Figure 1d-f).

The NSE ranges from 39.27% to 99.94% in calibration, and 77.62% to 97.91% in validation (Table 1). The lowest NSE values (39.27% and 59.06%) during calibration for W7-GC are due to wedge-shaped sediment peaks with step-like recession limbs, which the model cannot replicate precisely due to its smooth analytical structure. However, for both these events IFF-SMA-SGM effectively captures sediment peaks, with negligible $RE(Q_{PS})$ = 0.06% and 0.01%, while ensuring accurate sediment volume conservation ($RE(Q_S)$ = 0.00) over the actual time base. The model performs comparatively well in validation (NSE = 77.62%, $RE(Q_{PS})$ = 0.01%, $RE(Q_S)$ = 0.00) despite the oscillations in the recession limb of a sediment graph of W6-GC event, which the model doesn't replicate or follow, and the NSE get reduced. The *REs* for Q_S and Q_{PS} in the analysis range from 0.00% to 1.92%, and 0.01% to 5.96%, respectively. Most importantly, t_{PS} is predicted exactly in both calibration and validation ($RE(t_{PS})$ = 0.00), reinforcing the model's accuracy in replicating sediment graph shape, conserving sediment load, capturing peak sediment outflow and its timing over a given time base.

6. CONCLUSIONS

The proposed SGM effectively quantifies and partitions first-flush sediment load from the total observed sediment load. This capability allows for targeted identification, retention, treatment, disposal, and restoration of first-flush sediment, rather than treating runoff at a constant rate—reducing space and cost requirements. Additionally, first-flush estimates improve water quality sampling, optimize stormwater treatment infrastructure sizing, and refine BMP design, enhancing treatment efficiency while minimizing treatment volume and costs. The proposed SMA-based SGM accounts for first flush—influencing rainfall and climatic characteristics (antecedent dry weather conditions, rainfall depth, duration, and intensity) as well as catchment attributes (size and land use), making it physically more robust than conventional SGMs.

The key findings of the study are:

1. Integrating rainstorm-generated first-flush into the model improves the accuracy and reliability of sediment yield predictions. It enables cost-effective stormwater treatment planning by efficiently collecting and managing highly turbid primary sediment loads, reducing storage and maintenance needs.
2. The IFF-SMA-SGM accurately predicts temporal sediment rates, demonstrating its ability to capture physical processes governing sediment outflow at storm onset. Unlike conventional models, IFF-SMA-SGM explicitly accounts for the first-flush effect, initial abstraction, and initial soil moisture making it more effective and physically meaningful.
3. The hydrologically enhanced IFF-SMA-SGM reliably models sediment peaks while conserving mass, as evidenced by low *RE* values: $RE(Q_S)$ = 1.92%, $RE(Q_{PS})$ = 5.96% and $RE(t_{PS})$ = 0.00.
4. The proposed IFF-SMA-SGM significantly outperforms conventional SYMs and SGMs, which exhibit higher errors in Q_{PS} and Q_S:

Table 2 Observed error values in the application of conventional SYMs and SGMs.

Model	$RE(Q_{PS})$	$RE(Q_S)$
Kothyari et al. (1996)	56.63%	89.06%
Kothyari et al. (2002)	91.48%	87.74%
Rai and Mathur (2007)	61.5%	37.8%
Tyagi et al. (2008)	24.86%	42.15%
Singh et al. (2008)	12.95%	15.75%
Bhunya et al. (2010)	16.56%	10.04%
Gupta et al. (2019): Bhunya et al. (2010)	55.98%	66.95%
Present IFF-SMA-SGM	5.96%	1.92%

Furthermore, since many conventional models lack proper validation, the proposed approach—supported by rigorous validation—demonstrates greater reliability and accuracy.

5. By defining *SDR*-based constraints for estimating the event specific magnitude of *A*, and using *CN* to determine *S*, the average values of calibrated parameters (α, β, k, θ,

λ, and λ_1) (Table 1) are applicable for computing sediment rates in hydrologically similar ungauged watersheds, as demonstrated in the W14-GC validation.

6. The parameter-driven model complexity is eliminated by obviating the need for direct calibration/optimization of *A* and *S* and thus maintains the uniqueness and consistency of the rest of the model parameters (α, β, k, θ, λ, and λ_1) with literature-based estimates.
7. The study confirms the effectiveness of IFF-SMA-SGM in predicting total sediment loss and its temporal distribution, particularly for ungauged watersheds considering first-flush dynamics.
8. While the proposed method has proven effective in analyzing first-flush sediment dynamics for the investigated site, further validation under diverse hydrological and climatic conditions is necessary to fully assess its applicability and standardize the introduced first-flush coefficient.

Thus, IFF-SMA-SGM provides a physically robust, hydrologically sound, and computationally efficient framework for sediment yield modeling, outperforming existing approaches while ensuring practical applicability in watershed management.

ACKNOWLEDGMENTS

The authors wish to thank Graphic Era (Deemed to be University) Dehradun; and NIH, Roorkee, India for providing necessary research facilities and guidance as well.

REFERENCES

Aksoy, H., and M.L. Kavvas. 2005. "A Review of Hillslope and Watershed Scale Erosion and Sediment Transport Models." *Catena* 64 (2–3): 247–271. https://doi.org/10.1016/j.catena.2005.08.008

Australia EPA. 2006. “Storm Water First Flush Pollution.” http://www.epa.nsw.gov.au/

Bach, P.M., D.T. McCarthy, and A. Deletic. 2010. “Redefining the Stormwater First Flush Phenomenon.” *Water Research* 44 (8): 2487–2498. https://doi.org/10.1016/j.watres.2010.01.022

Barbosa, A.E. 1999. “Highway Runoff Pollution and Design of Infiltration Ponds for Pollutant Retention in Semi-Arid Climates.” Ph.D. Thesis, Environmental Engineering Lab., Aalborg University, Denmark.

Barco, J., S. Papiri, and M.K. Stenstrom. 2008. “First-flush in a Combined Sewer System.” *Chemosphere* 71 (5): 827–833. https://doi.org/10.1016/j.chemosphere.2007.11.049

Batista, P.V., J. Davies, M.L. Silva, and J.N. Quinton. 2019. “On the Evaluation of Soil Erosion Models: Are We Doing Enough?” *Earth-Science Reviews* 97, 102898. https://doi.org/10.1016/j.earscirev.2019.102898

Bennett, J.P. 1974. “Concepts of Mathematical Modeling of Sediment Yield.” *Water Resources Research* 10 (3): 485–492. https://doi.org/10.1029/WR010i003p00485

Bertrand-Krajewski, J., G. Chebbo, and A. Saget. 1998. “Distribution of Pollutant Mass vs. Volume in Stormwater Discharges and the First Flush Phenomenon.” *Water Research* 32 (8): 2341–2356. https://doi.org/10.1016/S0043-1354(97)00420-X

Bhunya, P.K., S.K. Jain, P.K. Singh, and S.K. Mishra. 2010. “A Simple Conceptual Model of Sediment Yield.” *Water Resources Management* 2 (8): 1697–1716. https://doi.org/10.1007/s11269-009-9520-4

Bhunya, P.K., S.K. Mishra, and R. Berndtsson. 2003. “Simplified Two Parameters Gamma Distribution for Derivation of Synthetic Unit Hydrograph.” *Journal of Hydraulic Engineering* 8 (4): 226–230. https://doi.org/10.1061/(ASCE)1084-0699(2003)8:4(226)

Blöschl, G., and M. Sivapalan. 1995. “Scale Issues in Hydrological Modeling: A Review.” *Hydrological Processes* 9 (3–4): 251–290. https://doi.org/10.1002/hyp.3360090305

Borrelli, P., C. Alewell, P. Alvarez, J.A.A. Anache, J. Baartman, C. Ballabio, N. Bezak, et al. 2021. “Soil erosion modeling: A global review and statistical analysis.” *Science of the Total Environment* 780, 146494. https://doi.org/10.1016/j.scitotenv.2021.146494

Bruce, R.R., L.A. Harper, R.A. Leonard, W.M. Snyder, and A.W. Thomas. 1975. “A Model for Runoff of Pesticides from Small Upland Watersheds.” *Journal of Environmental Quality* 4 (4): 541–548. https://doi.org/10.2134/jeq1975.00472425000400040024x

Chen, X.Y., and K.W. Chau. 2016. “A Hybrid Double Feed Forward Neural Network for Suspended Sediment Load Estimation.” *Water Resources Management* 30 (7): 2179–2194. https://doi.org/10.1007/s11269-016-1281-2

Chow, V.T. 1964. *Handbook of Applied Hydrology.* New York: McGraw-Hill.

Chui, P.C. 1997. “Characteristics of Stormwater Quality from Two Urban Watersheds in Singapore.” *Environmental Monitoring and Assessment 44*, 173–181. https://doi.org/10.1023/A:1005776321684

Deletic, A. 1998. “The First Flush Load of Urban Surface Runoff.” *Water Research* 32, 2462–2470. https://doi.org/10.1016/S0043-1354(97)00470-3

Favis-Mortlock, D.T., J. Boardman, A.J. Parsons, and B. Lascelles. 2000. “Emergence and Erosion: A Model for Rill Initiation and Development.” *Hydrological Processes* 14, 2173–2205. https://doi.org/10.1002/1099-1085(20000815/30)14:11/12<2173::AID-HYP61>3.0.CO;2-6

Fitzgerald, S.A., J.V. Klump, P.W. Swarzenski, R.A. Mackenzie, and K.D. Richards. 2001. “Beryllium-7 as a Tracer of Short-Term Sediment Deposition and Resuspension in the Fox River, Wisconsin.” *Environmental Science and Technology* 35, 300–305. https://doi.org/10.1021/es000951c

Gracia-Sánchez, J. 1996. “Generation of Synthetic Sediment Graphs.” *Hydrological Processes* 10 (9): 1181–1191. https://doi.org/10.1002/(SICI)1099-1085(199609)10:9<1181::AID-HYP369>3.0.CO;2-X

Graf, W.H. 1984. *Hydraulics of Sediment Transport*. Colorado, USA: Water Resources Publications LLC.

Gupta, K., and A.J. Saul. 1996. “Suspended Solids in Combined Sewer Flows.” *Water Science and Technology* 33 (9): 93–99. https://doi.org/10.1016/0273-1223(96)00374-5

Gupta, S.K., J. Tyagi, P.K. Singh, G. Sharma, and A.S. Jethoo. 2019. “Soil Moisture Accounting (SMA) Based Sediment Graph Models for Small Watersheds.” *Journal of Hydrology* 574, 1129–1151. https://doi.org/10.1016/j.jhydrol.2019.04.077

Hager, M. 2001. “Evaluating First Flush.” *Stormwater the Journal for Surface Water Quality Professionals* 2 (6).

Harmon, R.S., and W.W. Doe III. 2001. “Landscape Erosion and Evolution Modeling” New York: Kluwer Academic.

Hawkins, R.H., and A.V. Khojeini. 2000. “Initial Abstraction and Loss in the Curve Number Method.” *Hydrology and Water Resources in Arizona and the Southwest* 30. https://repository.arizona.edu/handle/10150/296552

Horton, R.E. 1939. “The Interpretation and Application of Runoff Plot Experiments with Reference to Soil Erosion Problems.” *Soil Science Society of America Journal* 3 (C): 340–349. https://doi.org/10.2136/sssaj1939.036159950003000C0066x

Hrissanthou, V. 1998. “Comparison between Two Mathematical Models for the Computation of Sediment Yield from a Basin.” *IAHS Publication No.* 249, 137–142.

Jakeman, A.J., R.A. Letcher, and J.P. Norton. 2006. “Ten Iterative Steps in Development and Evaluation of Environmental Models.” *Environmental Modeling and Software* 21 (5): 602–614. https://doi.org/10.1016/j.envsoft.2006.01.004

Jetten, V., A.D. De Roo, and D. Favis-Mortlock. 1999. “Evaluation of Field-Scale and Catchment-Scale Soil Erosion Models.” *Catena* 37 (3–4): 521–541. https://doi.org/10.1016/S0341-8162(99)00037-5

Johnson, J.W. 1943. “Distribution Graphs of Suspended-Matter Concentration.” *Transactions of the ASCE* 108 (1): 941–956. https://doi.org/10.1061/TACEAT.0005615

Jones, K.R., O. Berney, D.P. Carr, and E.C. Barrett. 1981. “Arid Zone Hydrology.” *FAO Rome, Irrigation and Drainage Paper No. 37* (34816): 370.

Karydas, C.G., P. Panagos, and I.Z. Gitas. 2014. “A Classification of Water Erosion Models According to their Geospatial Characteristics.” *International Journal of Digital Earth* 7 (3): 229–250. https://doi.org/10.1080/17538947.2012.671380

King, K.W., J.G. Arnold, and R.L. Bingner. 1999. "Comparison of Green-Ampt and Curve Number Methods on Goodwin Creek Watershed Using SWAT." *Transactions of the ASAE* 42 (4): 919–926. https://doi.org/10.13031/2013.13272

Kothyari, U.C., M.K. Jain, and K.G. Ranga Raju. 2002. "Estimation of Temporal Variation of Sediment Yield Using GIS." *Hydrological Sciences* 47 (5): 693–706. https://doi.org/10.1080/02626660209492974

Kothyari, U.C., A.K. Tiwari, and R. Singh. 1996. *“*Temporal Variation of Sediment Yield.” *Journal of Hydrologic Engineering* 1 (4): 169–176. https://doi.org/10.1061/(ASCE)1084-0699(1996)1:4(169)

Krebs, P., P. Holzer, J.L. Huisman, and W. Rauch. 1999. "First Flush of Dissolved Compounds." *Water Science and Technology* 39 (9): 55–62 https://doi.org/10.1016/S0273-1223(99)00216-4

Kuhnle, R.A., R.L. Bingner, C.V. Alonso, C.G. Wilson, and A. Simon. 2008. "Conservation Practice Effects on Sediment Load in the Goodwin Creek Experimental Watershed." *Journal of Soil and Water Conservation* 63 (6): 496–503.

Kuhnle, R.A., and D.G. Wren. 2003. "Breakout session I, Suspended Sediment Measurement: Data Needs, Uncertainty, and New Technologies." In *Proceedings of the Federal Interagency Sediment Monitoring Instrument and Analysis Research Workshop* 1276, 8–15.

Kumar, S., and R.A. Rastogi. 1987. "A Conceptual Catchment Model for Estimating Suspended Sediment Flow." *Journal of Hydrology* 95 (1–2): 155–163. https://doi.org/10.1016/0022-1694(87)90122-3

Larsen, T., K. Broch, and M.R. Andersen. 1998. “First Flush Effects in an Urban Catchment Area in Aalborg.” *Water Science and Technology* 37 (1): 251–257. https://doi.org/10.1016/S0273-1223(97)00776-2

Lasdon, L.S., A.D. Waren, A. Jain, and M. Ratner. 1978. “Design and Testing of A Generalized Reduced Gradient Code For Nonlinear Programming.” *ACM Transactions on Mathematical Software* 4 (1): 34–50.

Lee, K.T., and C.C. Yang. 2010. "Estimation of Sediment Yield During Storms Based on Soil and Watershed Geomorphology Characteristics." *Journal of Hydrology* 382 (1-4): 145–153. https://doi.org/10.1016/j.jhydrol.2009.12.025

Lee, Y.H., and V.P. Singh. 1999. "Prediction of Sediment Yield by Coupling Kalman Filter with Instantaneous Unit Sediment Graph." *Hydrological Processes* 13 (17): 2861–2875. https://doi.org/10.1002/(SICI)1099-1085(19991215)13:17<2861::AID-HYP805>3.0.CO;2-Z

Lee, Y.H., and V.P. Singh. 2005. "Tank Model for Sediment Yield." *Water Resources Management* 19, 349–362. https://doi.org/10.1007/s11269-005-7998-y

Li, L.Q., C.Q. Yin, Q.C. He, and L.L. Kong. 2007. “First flush of Storm Runoff Pollution from an Urban Catchment in China.” *Journal of Environmental Sciences* 19 (3): 295–299. https://doi.org/10.1016/S1001-0742(07)60048-5

Maestri, B., M.E. Dorman, and J. Hartigan. 1988. “Managing Pollution from Highway Storm Water Runoff. *Transportation Research Record* 1166, 15–21.

Mein, R.G., and C.L. Larson. 1971. “Modeling the Infiltration Component of the Rainfall-Runoff Process.” Minneapolis University of Minnesota.

Merritt, W.S., R.A. Letcher, and A.J. Jakeman. 2003. “A Review of Erosion and Sediment Transport Models.” *Environmental Modeling and Software* 18 (8–9): 761–799. https://doi.org/10.1016/S1364-8152(03)00078-1

Metcalf, L., and H.P. Eddy. 1915. *American Sewerage Practice Volume III: Disposal of Sewage.* New York: McGraw-Hill Inc.

Michel, C., V. Andréassian, and C. Perrin. 2005. "Soil Conservation Service Curve Number Method: How to mend a wrong soil moisture accounting procedure?" *Water Resources Research* 41 (2): 1–6. https://doi.org/10.1029/2004WR003191

Mishra, S.K., and V.P. Singh. 2003. *Soil Conservation Service Curve Number (SCS-CN) Methodology*. Kluwer Academic: Dordrecht, The Netherlands.

Mishra, S.K., J.V. Tyagi, V.P. Singh, and R. Singh. 2006. "SCS-CN-Based Modeling of Sediment Yield." *Journal of Hydrology* 324 (1–4): 301–322. https://doi.org/10.1016/j.jhydrol.2005.10.006

Mizumura, K. 1989. “Hydrological Approach to Prediction of Sediment Yield.” *Journal of Hydraulic Engineering* 115 (4): 529–535. https://doi.org/10.1061/(ASCE)0733-9429(1989)115:4(529)

Nash, J.E. 1957. "The Form of the Instantaneous Unit Hydrograph." *International Association of Hydrological Sciences General Assembly, Toronto* 3, 114–121. https://nora.nerc.ac.uk/id/eprint/508550

Novotny, V. 1980. “Delivery of suspended sediment and pollutants from non-point sources during overland flow.” *JAWRA Journal of the American Water Resources Association* 16 (6): 1057–1065.

Novotny, V., D. Balsiger, R. Bannerman, J.G. Konrad, D.S. Cherkauer, G.V. Simsiman, and G. Chesters. 1979. “Simulation of Pollutant Loadings and Runoff Quality. EPA 905/4-79-029, USEPA.”

Novotny, V., and G. Chesters. 1981. *Handbook of Nonpoint Pollution: Sources and Management.* Van Nostrand Reinhold Environmental Engineering Series (USA).

Novotny, V., and H. Olem. 1994. *Water Quality: Prevention, Identification and Management of Diffuse Pollution.* New York: Van Nostrand Reinhold, 18–25.

Novotny, V., G.V. Simsiman, and G. Chesters. 1986. “Delivery of Pollutants From Nonpoint Sources.” *IAHS-AISH Publication* 159, 133–140.

Perrin, C., C. Michel, and V. Andréassian. 2003. “Improvement of a Parsimonious Model for Streamflow Simulation.” *Journal of Hydrology* 279 (1–4): 275–289. https://doi.org/10.1016/S0022-1694(03)00225-7

Pilgrim, D.H., T.G. Chapman, and D.G. Doran. 1988. "Problems of Rainfall-Runoff Modeling In Arid and Semiarid Regions." *Hydrological Sciences Journal* 33 (4): 379–400. https://doi.org/10.1080/02626668809491261

Ponce, V.M., and R.H. Hawkins. 1996. "Runoff Curve Number: Has it Reached Maturity?" *Journal of Hydrologic Engineering* 1 (1): 11–19. https://doi.org/10.1061/(ASCE)1084-0699(1996)1:1(11)

Rai, R.K., and B.S. Mathur. 2007. "Event-based Soil Erosion Modeling of Small Watersheds." *Journal of Hydrologic Engineering* 12 (6): 559572. https://doi.org/10.1061/(ASCE)1084-0699(2007)12:6(559)

Raghuwanshi, N.S., R.A. Rastogi, and S. Kumar. 1994. "Instantaneous-unit Sediment Graph." *Journal of Hydraulic Engineering* 120 (4): 495–503. https://doi.org/10.1061/(ASCE)0733-9429(1994)120:4(495)

Reid, I., and L.E. Frostick. 1987. "Flow Dynamics and Suspended Sediment Properties in Arid Zone Flash Floods." *Hydrological Processes* 1 (3): 239–253. https://doi.org/10.1002/hyp.3360010303

Renard, K.G., and E.M. Laursen. 1975. "Dynamic Behavior Model of Ephemeral Stream." *Journal of the Hydraulics Division* 101 (5): 511–528. https://doi.org/10.1061/JYCEAJ.0004340

Rendon-Herrero, O. 1978. “Unit Sediment Graph.” *Water Resources Research* 14 (5): 889–901. https://doi.org/10.1029/WR014i005p00889

Roehl, J.E. 1962. “Sediment Source Areas, and Delivery Ratios Influencing Morphological Factors.” *International Association of Hydrological Sciences* 59, 202–213.

Saget, A., G. Chebbo, and J.L. Bertrand-Krajewski. 1996. “The First Flush in Sewer Systems.” *Water Science and Technology* 33 (9): 101–108.

Sansalone, J.J. 2005. “The Rise and Fall of Best Management Practices: The Coming Age of Unit Operations and Process Concepts for Storm Water.” *Proceedings of TRB Symposium, Florida.*

Sansalone, J.J., and S.G. Buchberger. 1996. "Characterization of Metals and Solids in Urban Highway Winter Snow and Spring Rainfall-Runoff." *Transportation Research Record* 1523 (1): 147–159. https://doi.org/10.1177/0361198196152300118

Sansalone, J.J., and C.M. Cristina. 2004. "First Flush Concepts for Suspended and Dissolved Solids in Small Impervious Watersheds." *Journal of Environmental Engineering* 130 (11): 1301–1314. https://doi.org/10.1061/(ASCE)0733-9372(2004)130:11(1301)

Schiffer, D.M. 1989. "Water-quality Variability in a Central Florida Wetland Receiving Highway Runoff." *Water: Laws and Management.* American Water Resources Association, Bethesda, Maryland 7A: 1–11.

SCS. 1972. *National Engineering Handbook, Section 3-4.* U.S. Department of Agriculture: Washington, D.C.

Sharma, K.D., R.P. Dhir, and J.S.R. Murthy. 1992. "Modeling Suspended Sediment Flow in Arid Upland Basins." *Hydrological Sciences Journal* 37 (5): 481–490. https://doi.org/10.1080/02626669209492613

Sharma, K.D., and J.S.R. Murthy. 1996. "A Conceptual Sediment Transport Model for Arid Regions." *Journal of Arid Environments* 33 (3): 281–290. https://doi.org/10.1006/jare.1996.0065

Singh, P.K., P.K. Bhunya, S.K. Mishra, and U.C. Chaube. 2008. "A Sediment Graph Model Based on SCS-CN Method." *Journal of Hydrology* 349 (1–2): 244–255. https://doi.org/10.1016/j.jhydrol.2007.11.004

Singh, V.P., A. Baniukiwicz, and V.J. Chen. 1982. "An Instantaneous Unit Sediment Graph Study for Small Upland Watersheds." *Applied Modeling in Catchment Hydrology*, 539–554.

Stahre, P., and B. Urbonas. 1990. *Stormwater Detention*. Englewood Cliffs, New Jersey: Prentice Hall, Inc. 338.

Stenstrom, M.K., S.L. Lau, H.H. Lee, J.S. Ma, H. Ha, L.H. Kim, S. Khan, and M. Kayhanian. 2001. "First Flush Stormwater Runoff From Highways." In *Bridging the Gap: Meeting the World's Water and Environmental Resources Challenges,* 1–10. https://doi.org/10.1061/40569(2001)178

Su, Y., and G.F. Mitchell. 2003. "Using First Order Modeling to Describe First Flush Effects of Storm Water Runoff." *Proceedings of American Surface Water Quality Conference and Expo.* San Antonio, TX.

Tyagi, J.V., S.K. Mishra, R. Singh, and V.P. Singh. 2008. "SCS-CN based Time-Distributed Sediment Yield Model." *Journal of Hydrology* 352 (3–4): 388–403. https://doi.org/10.1016/j.jhydrol.2008.01.025

Wanielista, M.P., and Y.A. Yousef. 1993. *Stormwater Management*. New York: John Wiley and Sons, Inc.

Williams, J.R. 1978. "A Sediment Graph Model Based on an Instantaneous Unit Sediment Graph." *Water Resources Research* 14 (4): 659–664. https://doi.org/10.1029/WR014i004p00659

Wilson, C.G., R.A. Kuhnle, D.D. Bosch, J.L. Steiner, P. Starks, M.D. Tomer, and G.V. Wilson. 2008. "Quantifying Relative Contributions from Sediment Sources in Conservation Effects Assessment Project Watersheds." *Journal of Soil and Water Conservation* 63 (6): 523–532. https://doi.org/10.2489/jswc.63.6.523

Wischmeier, W.H., and D.D. Smith. 1978. *Predicting Rainfall Erosion Losses: A Guide to Conservation Planning. No. 537.* Washington, D.C.: U.S. Department of Agriculture, Science and Education Administration.

Woodward, D.E., R.H. Hawkins, R. Jiang, A.T. Hjelmfelt, Jr, J.A. Van Mullem, and Q.D. Quan. 2003. "Runoff curve Number Method: Examination of the Initial Abstraction Ratio." *World Water and Environmental Resources Congress* 1–10.